Bull. Mater. Sci., Vol. 39, No. 3, June 2016, pp. 865–874. © Indian Academy of Sciences.
DOI 10.1007/s12034-016-1200-4

Adsorption of hexavalent chromium by graphite–chitosan binary composite

RAJENDRA S DONGRE
Department of Chemistry, RTM Nagpur University, Nagpur 440033, India

MS received 28 February 2015; accepted 18 December 2015

Abstract. **Graphite chitosan binary (GCB) composite was prepared for hexavalent chromium adsorption from studied water. GCB was characterized by TGA, FTIR, SEM and X-ray diffraction techniques. Wide porous sorptive surface of 3.89 $m^2\ g^{-1}$ and absorptive functionalities of GCB was due to 20% (w/w) graphite support on chitosan evidenced from FTIR and SEM that impart maximum adsorption at pH 4, agitation with 200 rpm for 180 min. Adsorption studies revealed intraparticle diffusion models and best-fitted kinetics was pseudo 2nd order one. A well-fitted Langmuir isotherm model suggested monolayer adsorption with an adsorption capacity (q_m) of 105.6 mg g^{-1} and $R^2 = 0.945$. Sorption mechanisms based on metal ionic interactions, intrusion/diffusion and chemisorptions onto composite. This graphite chitosan binary composite improve sorbent capacity for Cr(VI).**

Keywords. **Hexavalent chromium; graphite–chitosan composite; adsorption kinetics.**

1. Introduction

Release of heavy metal in water is a threat to environment and health due to their carcinogenic and mutagenic toxicity [1]. Among heavy metals, chromium is non-biodegradable, bio-available and persists as trivalent and hexavalent species. Cr(VI) moves readily via soils and water appeared more toxic as it causes lung cancer, besides absorption through skin [2], while Cr(III) is less toxicity and relatively innocuous. Cr(VI) generates in waste streams from paints, textile, dyeing, electroplating, metal finishing, power generation, electronic device, leather-tanneries, flyash incinerators, mining, radioactive materials, batteries and pesticides [3]. Environmental protection agency (EPA) ascertained Cr(VI) limit level for surface water discharge about 100 ppb and in potable water is 50 ppb [4].

Metal contamination can be treated by techniques viz., precipitation; coagulation, adsorption, extraction, ion-exchange, electro-chemical, ultra-filtration and reverse osmosis, etc [5]. These techniques are costly and possess incomplete removal, huge sludge production (disposal problems) and needs quantitative reagent with energy input. Nonetheless, activated carbon used adsorption is effective; but an expensive process to remove chromium [6].

Biopolymers used in metal biosorption found to be superior to adsorption, as viability unaffected by metal uptake and very effective method [7]. Chitin, chitosan and cellulose biopolymer resources are environment-friendly and widely available/agriculture wastes/seafood processing [8]. Recently, chitosan blend with cellulose/glass ceramic/alumina/silica yield composites/hybrids alteration via functionalization and cross-sectional/morphological changes to enhance its adsorption capacity [9,10]. Ubiquitous, after cellulose found in fungi, chitin is 2nd abundant insects, crustaceans and invertebrates as *N*-acetyl-2-amino-2-desoxy-polysaccharide linked (β1–4) glycosidic framework [11]. Chitosan has oligosaccharides of 2 to 20 units similar to cellulose (except at C-2 position O=C–NH_2 instead of –OH). Weak chemical properties of chitosan can be overcome by surface modification/chemical treatments [12] to articulate –NH_2/–OH proactive groups for dyes adsorption [13] or metal complextion/diffusion in accessible pore size [14]. In this contest, graphite's hexagonal layers that are well-utilized in heat-resistant/reinforced material [15,16] were exploited to yield inter-wined binary composite for Cr(VI) removal are developed.

2. Experimental

2.1 *Material and methods*

All chemicals were AR grade. Chitosan purchased from Sisco Lab, Mumbai (India) and graphite procured from Loba Chemie, Mumbai (India). Acetic acid (99.5%, Merck) and ammonium hydroxide (30%, Merck) are used. Digital pH meter (Hanna) used and standardized using buffer of pH 4 and 9 (Fisher Scientific) and pH adjustment done by 0.1 N HCl/NaOH (Fisher Scientific) and Rotary Shaker (Remi make) were used.

2.2 *Synthesis of graphite chitosan binary composite (GCB)*

GCB is synthesized by impregnation method. Chitosan dissolved in 3% acetic acid and warmed at 50°C to obtain gel

rsdongre@hotmail.com

and then graphite (20%, w/w) added and stirred magnetically at NTP for 5–6 h and resultant was sprayed by a syringe in 50% aqueous ammonia to obtain beads. Finally, beads filtered, washed with distilled water to remove dirt, particulate matter or any colour and dried in oven at 90–105°C for 24 h. The beads were grounded in mortar pestle and sieved to get particle size of 175–245 μm (stored in PVC bottles). Cr(VI) stock solution (1000 mg l^{-1}) prepared by dissolving potassium dichromate in double-distilled water and diluted in concentration range of 5–100 mg l^{-1}.

2.3 *Instrumentations and equipments*

Fourier transform infrared (FTIR) performed using Perkin Elmer cast in disks–KBr pellets (450–4000 cm^{-1}) and XRD on Rigaku MiniFlex-2 Goniometer using CuKα (30 kV, 15 mA). SEM done at accelerating voltage of 15 kV at magnification range of 20 to 5000× using JSM 6380. Brunauer-Emmett-Teller (BET) surface area was measured using Micromeritics ASAP-2020 V3-04 H. Elemental contents estimated by C/H/N/S analyzer Vario El Cube at 230 V.

2.4 *Analysis of Cr(VI) ions by spectrophotometer*

Cr(VI) residual concentration after adsorption determined by UV–VIS spectrophotometer (7400CE CECIL) at 540 nm by 1,5 diphenylcarbazide method [17].

2.5 *Batch adsorption studies of graphite chitosan binary (GCB) composite*

Bath adsorption for Cr(VI) ion 100 ml solution taken in 250 ml Erlenmeyer flasks with suitable amount of adsorbent shaken on rotary shaker followed by filtration using Whatman no.1. The supernatants were analysed for residual Cr(VI) ions after contact period of 15, 30, 60, 120, 180, 240, 300 and 360 min. pH effect on Cr(VI) sorption studied in pH 2–9 range with GBC at 50–500 ppm. Adsorption isotherms were studied in Cr(VI) range of 20–100 ppm with adsorbent dose of 50 ppm. Langmuir and Freundlich models were studied.

2.6 *Characterizations*

2.6a *Elementary analysis (viz., C/H/N/S/O, % ash, % moisture, surface parameters)*: Elementary analysis of chitosan, graphite and GCB composite are shown in table 1. Ash content determined by known method [18] and calculated by equation (1), % moisture by gravimetry [19] and water mass/weight difference of wet and dried samples are calculated by equation (2):

$$\%\ \text{Ash} = \left[\text{weight of residue (g)/sample weight (g)}\right] \times 100 \quad (1)$$

$$\%\ \text{Moisture content} = [\text{wet weight (g)} - \text{dry weight (g)}]/\text{wet weight (g)} \times 100. \quad (2)$$

2.6b *Infrared spectra*: The free amino and hydroxyl groups get protonated in acidic medium to form (NH_3^+ and OH_2^+), those are capable for Cr(VI) sorption by charge neutralization [20]. Hence, GBC composite was analysed by FTIR before and after adsorption as shown in figure 1c–d.

The metal ion Cr(VI) exists as anionic $HCrO_4^-$ form at pH 4, hence gets strongly adsorbed by chitosan-adsorbent GBC. The main adsorption peak of chitosan-absorbent GBC after adsorption found at 1382 cm^{-1} that remain unchanged before adsorption (figure 1b, c). This is due to physical adsorption of Cr(VI) and not a complexing reaction as reported on cross-linked chitosan beads [21]. Chitosan IR at 3695 cm^{-1},

Table 1. Characteristics of chitosan, graphite chitosan binary composite (GBC).

Analysed parameters	GCB	Pure chitosan	Graphite
Ash on ignition (800°C)	4.0%	2.10%	<1.0%
C%	59.35%	42.62%	>94%
H%	3.9%	7.73%	4%
N%	3.29%	7.98%	Nil
S%	0.155%	0.155%	Nil
O%	33.3%	33.3%	0.001%
Moisture	1.0%	2.90%	Nil
Volatile matter	55%	55%	Nil
Fixed carbon	33.80%	42.62%	95%
Particle size	176–246 μm	75–100 mm	50–75 μm
Density (g cm^{-3})	0.988 (g cm^3)	0.20–0.30 (g cm^{-3})	2.25
Viscosity	Crystalline particles	250–600 mPa (1% solution)	Non-viscous
Appearance/colour	Dirty white/ash colour	Off-white	Iron-black; luster
Solubility	Insoluble in solvents	1% acetic acid	Ethanol <0.2%
Surface area (m^2 g^{-1}) (BET)	3.890 m^2 g^{-1}	2.89 m^2 g^{-1}	8.0–12.0 m^2 g^{-1}
Total pore volume (cm^3 g^{-1})	0.002	0.014	0.1–0.3 P/P0
Mean pore diameter (nm)	28.12	10.40	—

3073 cm^{-1} and 2800–2950 cm^{-1} assigned for –OH stretching, while at 1667 cm^{-1} due to C=O stretching in amide and at 1152 cm^{-1} for bridge-O-stretching. The IR bands at 1262 cm^{-1} attributed for C–O–H stretching and broad IR at 1077 cm^{-1} to ring vibrations of C–O–H, C–O–C and CH_2OH [22]. IR at 1667 cm^{-1} for chitosan, amide disappeared in GBC and remarkably shifted to 1367 cm^{-1} of chitosan. IR chitosan as of mixed morphological changes reflected due to blend with

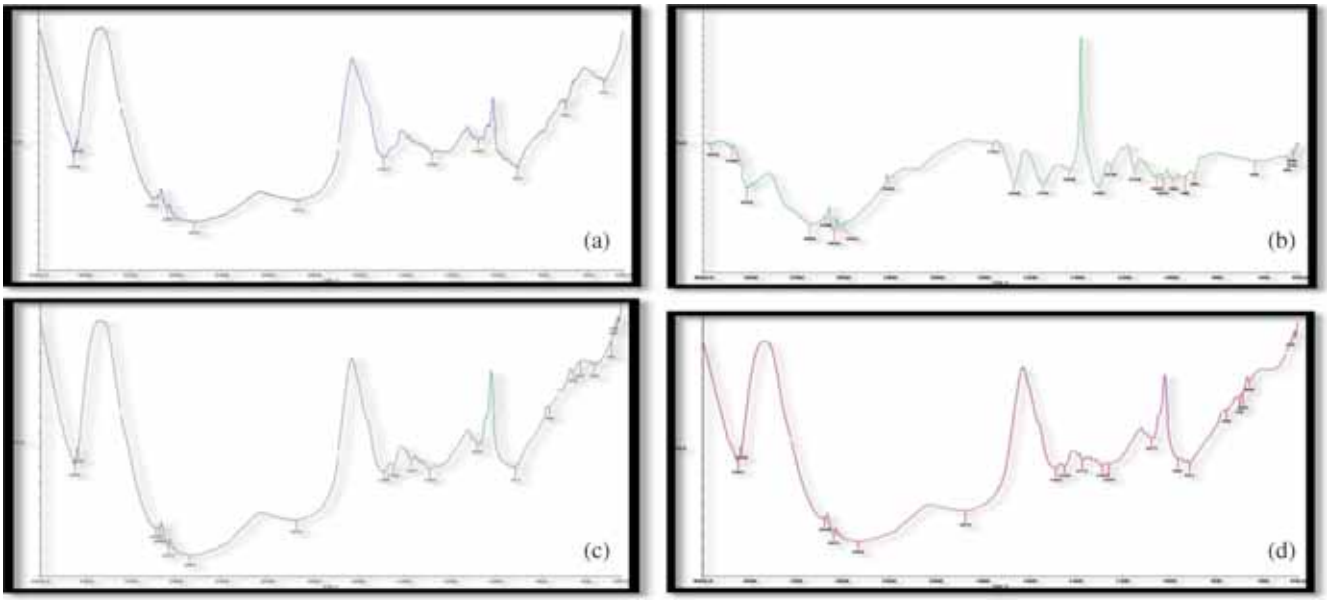

Figure 1. FTIR of (**a**) graphite, (**b**) chitosan, (**c**) GBC before and (**d**) after Cr(VI) adsorptions.

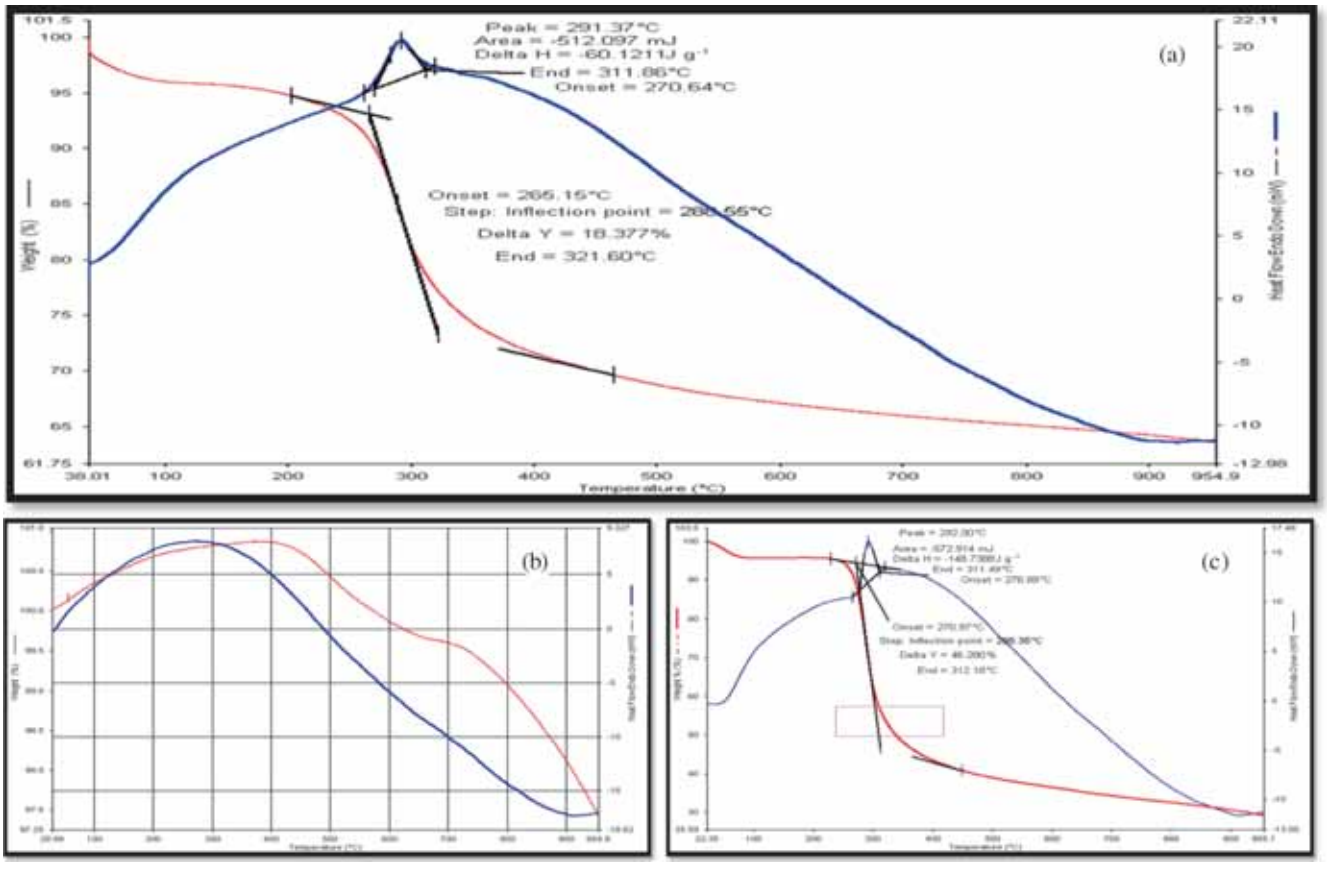

Figure 2. TGA of (**a**) graphite, (**b**) chitosan and (**c**) GBC composite.

graphite. After Cr(VI) uptake by GCB, the band shifted from 2872 to 2875 cm^{-1}, supports –OH link with Cr(VI) [20].

2.6c *Thermogravimetric analysis (TGA)*: TGA is used to determine decomposition temperature of materials. GBC composite exhibited 1st decomposition at 38°C which continued until 200°C with 5% weight loss due to evaporation of water and 2nd decomposition at 265.15°C and continued to 321.6°C with 18.37% weight chitosan loss and maximum degradation at 288.55°C, which ends at 954.9°C with total 35% weight loss of chitosan skeleton. Nevertheless, two exothermic peaks of GBC namely at 292 and 270.89°C, respectively, shown in figure 2c indicated less thermal stability of GBC composite than pure graphite, figure 2b, instead more stable than pure chitosan (figure 2c).

2.6d *Scanning electron microscope (SEM) analysis*: SEM well exhibits visual confirmation of physical state [23] and surface morphology of the graphite, chitosan and GCB composite to measure porosity and particle size dimensions. SEM images at magnifications show that chitosan microparticles are spherical with a slightly wrinkled surface and nonporous, uneven granular structure shown in figure 3c. SEM of graphite exhibited individual needle-shaped particles with intrinsic flake morphology shown in figure 3d. GCB composite SEM changes in crystal shape, morphology and agglomerated structure with particle size range of 175–246 μm (pore volume 28.12 nm) exhibited irregular surfaces and rugosity due to inter-wined/cross-linking and fractures different than non-homogenous chitosan surfaces shown in figure 3a and b. GCB entirely differs from chitosan and graphite as it supported solid reinforcement in chitosan and alter surface properties [24].

2.6e *XRD analysis*: XRD of chitosan, graphite and GCB composite are illustrated in figure 4a–c, respectively. Chitosan XRD exhibited broad diffraction peaks at $2\theta = 10$, 20.2 and 20.74° with d-spacing of 4.2 Å as characteristic fingerprints of semi-crystallinity [25] and no impurity peaks observed. GCB showed a diffraction peak at $2\theta = 26.5°$ (with d-spacing of about 3.35 Å) due to graphite reinforcement [26] indicated single phase composition. While GCB composite showed broad peak at $2\theta = 20°$ due to the chitosan decreased in intensity after doping with graphite and confirms reinforcement in chitosan. Broaden small peaks around $2\theta = 18-22°$ and a few peaks at $2\theta = 40$ and 44° in GCB showed successful inter-wined graphite layer in chitosan to provide an auxiliary surface support and a high degree of crystallinity [27].

3. Results and discussion

3.1 *Adsorption isotherms*

Langmuir and Freundlich models used for isothermal study as presented in table 2 and figures 5 and 6. The isotherms from regression analysis depicted Cr(VI) equilibrium at composite boundary.

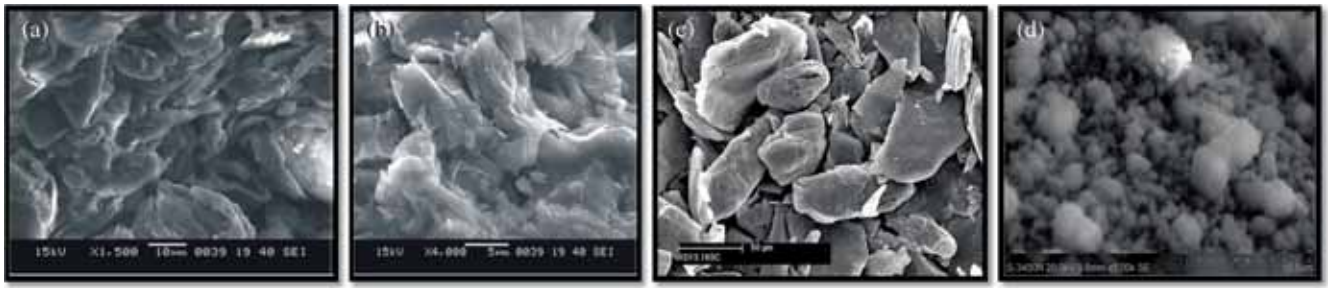

Figure 3. SEM images of GCB composite at (**a**) 1500×, (**b**) 4000×, (**c**) graphite at 250× and (**d**) chitosan skeleton at 5000×.

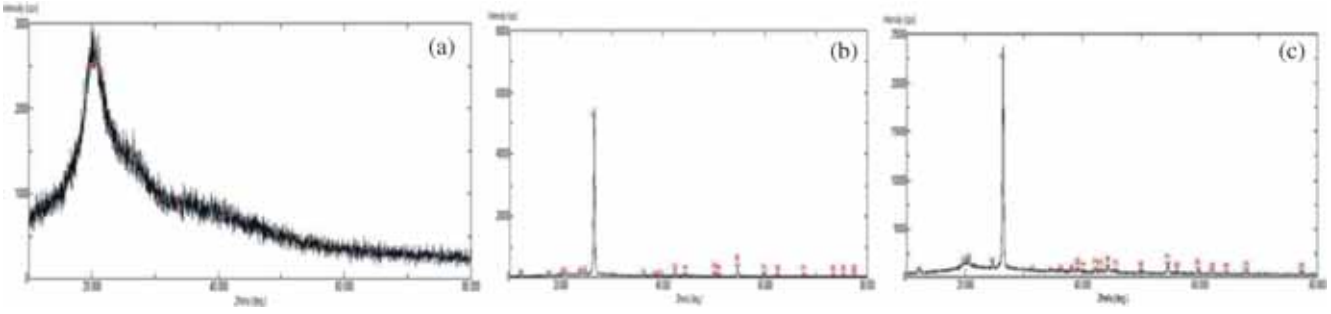

Figure 4. Powder XRD patterns of (**a**) chitosan, (**b**) graphite and (**c**) GCB composite.

Table 2. Linear equations, parameters for Cr(VI) adsorption onto GCB composite.

Equillibrium models	Langmuir constants					Freundlich constants		
Parameters	Q_{max} (mg g^{-1})	b (l mg^{-1})	R^2	k	R_L	K_f	$1/n$	R^2
Value	105	0.367	0.943	0.966	0.028–0.076	3.564	0.151	0.807

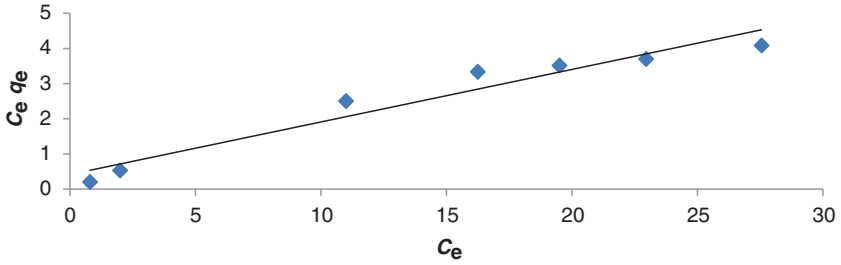

Figure 5. Langmuir adsorption isotherm.

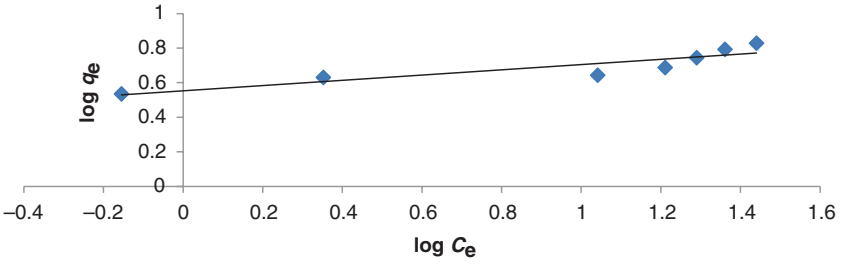

Figure 6. Freundlich adsorption isotherm.

R_L value expresses essential characteristics of isotherm model and defined by equation (3) given below:

$$\frac{C_e}{q_e} = \frac{1}{q_m K_L} + \frac{1}{q_m} C_e, \tag{3}$$

where C_e = concentration of Cr(VI) in solution at equilibrium (mg l^{-1}). q_e is the amount of Cr(VI) adsorbed at equilibrium (mg g^{-1}) and calculated by equation

$$q_e = (C_0 - C_e)V/m,$$

where C_0 is initial concentration of Cr(VI) in solution (mg l^{-1}), C_e is concentration of Cr(VI) in solution at equilibrium (mg l^{-1}), m is mass of adsorbent used (g) and V is volume of Cr(VI) solution (L) taken. Adsorption gets favourable if $0 < R_L < 1$ and for $R_L > 1$, it is unfavourable, but for $R_L = 1$ and $R_L = 0$, its linear and irreversible, respectively, [28] based on assumptions [29] that Cr(VI) are adsorbed at defined adsorbent sites and each site can hold single Cr(VI), besides all sites are equivalent in thermodynamics and kinetics. If initial Cr(VI) concentration rise, then adsorption enhanced till binding sites get saturated. R^2 and R_L in the range of 0–1 showed applicability/fit of Langmuir model. Adsorption capacity q_m and b (b = ratio of C_e/q_m, where q_m is maximum adsorption capacity of adsorbent) were 105 mg g^{-1} and 0.367 l mg^{-1}, respectively, for GCB composite compared with biosorbents in table 2 [30,31]. Adsorption capacity of chitosan for Cr(VI) reported 23 mg g^{-1} [32] under similar conditions.

3.2 *Kinetics of adsorption*

Adsorption is controlled by kinetics [32] and estimation of sorption rates guides sorption mechanisms. Thus, pseudo 1st and 2nd order kinetics intraparticle diffusion were investigated as given in equations (3–9) and shown in figures 7–9:

$$\ln\left(q_e - q_f\right) = \ln\ q_e - k_1 t \quad \text{pseudo 1st order model.} \tag{4}$$

Using equation (2), ln ($q_e - q_t$) *vs.* t plotted and pseudo 2nd order model, rate-limiting step is surface adsorption involved chemisorption, where removal of metal from solution is due to physicochemical interactions [32] as mentioned in figure 9. The kinetic parameters are calculated by equations (5–8).

$$(t/q_t) = (1/k_2/q_{e^2}) + (1/q_e t)\,, \tag{5}$$

$$\frac{1}{q_e} = \frac{1}{q} + \left(\frac{1}{k_2 q_{e^2}}\right)\frac{1}{t}, \tag{6}$$

$$q_e = q_t - \left(\frac{1}{k q_t}\right)\frac{q}{t}, \tag{7}$$

$$\frac{q_e}{t} = k q_t^2 - k q_e q_t. \tag{8}$$

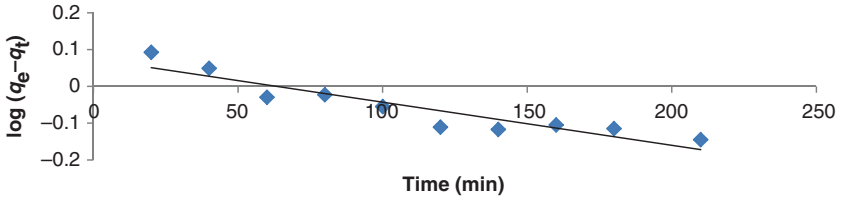

Figure 7. Pseudo first-order kinetic plot for removal of Cr(VI) by composite.

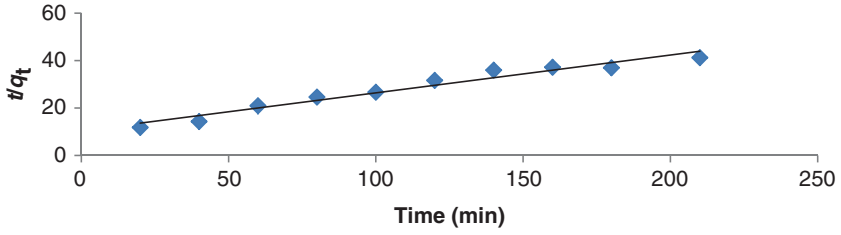

Figure 8. Pseudo second-order kinetic plot for removal of Cr(VI) by composite.

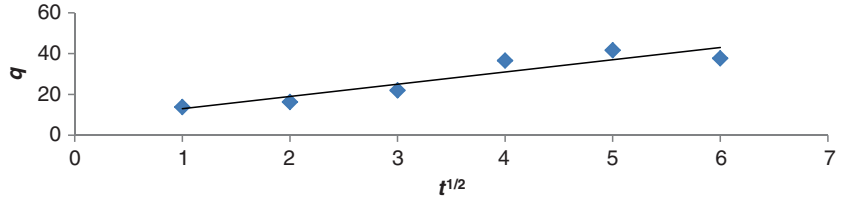

Figure 9. Intraparticle diffusion model kinetics for removal of Cr(VI) by composite.

The intraparticle diffusion model explains that adsorption depends on speed at which adsorbate/Cr(VI) diffuses towards composite (i.e., diffusion-controlled) presented in equation (9):

$$q_e = k_3 t^{1/2} + c, \tag{9}$$

where k_3 is a rate constant of intraparticle transport (g mg^{-1} min^{-1}) and c is intercept [33] and presented in figure 9. The adsorption equilibrium reached within 180 min, maximum 92% removal of Cr(VI) adsorbed with extremely slow diffusion from surface into pores, which were least accessible sites for adsorption [32]. The coefficient $R^2 = 0.95$ by pseudo 2nd order is higher than $R^2 = 0.93$, by pseudo 1st order and $R^2 = 0.91$ by intraparticle diffusion. Similarly, high k_2 obtained by pseudo 2nd order suggested rapid sequestered by composite functionalities results quick equilibrium. So, adsorbent/composite and adsorbate/Cr(VI) ratio are governing rate-determining step, suggested chemical adsorption/chemisorptions [32,33].

3.3 *Effect of pH*

Adsorption depends on ionic state of functionalities at the adsorbent's surface that gets changed with pH [34], thus, sorption studied in pH 2–9% Cr(VI) removal enhanced as pH raise from 2 to 5.5, and more removal under acid conditions

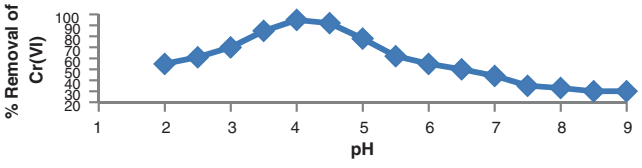

Figure 10. Effect of pH on % removal of Cr(VI) ions (initial concentration: 25 mg l^{-1}; temperature: 27°C; agitation speed: 200 rpm; contact time: 180 min; adsorbent dose: 5 g l^{-1}; pH 4).

is shown in figure 10. But, adsorption decreased at pH > 5.5 is considered as poor under basic conditions indicated characteristic chemisorptions due to few competitive protons sorption [32,35]. At acidic pH = 3–5.5, $HCrO_4^-$ and $Cr_2O_7^{2-}$ anions are predominant, but at acidic pH < 2.5, $Cr_3O_{10}^-$ and $Cr_4O_{13}^{2-}$ are dominated in equilibrium [35]. $HCrO_4^-$ anions interacted strongly with positive charges located on surface composites sites which get decreased at acidic pH < 2.5. Cr(VI) gets maximum adsorbed at pH 3.5–5.5 range, so, kept pH = 4 as optimum throughout. The electrostatic binding sites corresponding polymerized chromium anionic species decrease in basic pH, consequently adsorption gets decreased. Besides, at pH > 7, the composite surface gets negatively charged and subsequently enhanced electrostatic repulsion between Cr(VI) ions and charges at adsorbent sites, leads to release of adsorbed Cr(VI) off GCB composite [36].

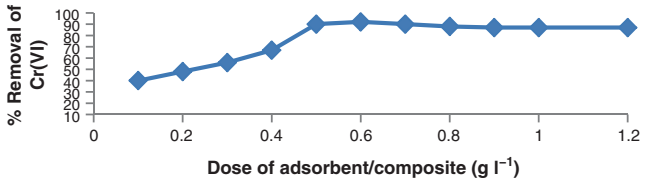

Figure 11. Effect of adsorbent dose on % removal of Cr(VI) (Cr(VI) concentration: 25 mg l^{-1}; temperature: 27°C; agitation: 200 rpm; contact time: 180 min; adsorbent dose: 5 g l^{-1}; pH 4).

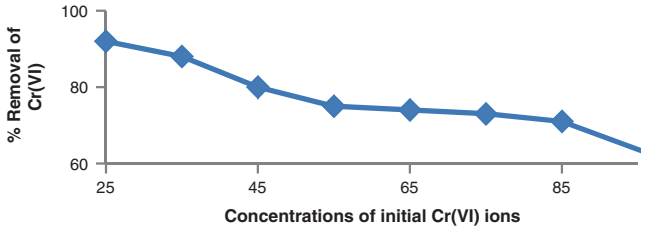

Figure 12. Effect of initial Cr(VI) ion concentration on % removal (temperature: 27°C; agitation: 200 rpm; contact time: 180 min; adsorbent dose: 5 g l^{-1}; pH 4).

3.4 *Effect of adsorbent dose (GCB)*

The % graphite functionalized on chitosan yields composite which differs adsorption capacity/efficiency with varying dose of GCB under the optimal conditions as illustrated in figure 11. As increase in GCB dosage from 0.1 to 0.6 g l^{-1}, removal efficiency augmented from 42 to 92% (49–105 mg g^{-1} for 5 mg l^{-1}). Adsorption efficiency rises due to availability of amino/hydroxyl proactive groups responsible for sorption and at lower dose metal : adsorbent ratio is decreased. Besides Cr(VI) removal is not linearly proportionate to increase in adsorbent dose (>0.6 g l^{-1}), instead remains steady, as attributed to interference between binding sites [37].

3.5 *Effect of initial Cr(VI) concentration*

Effects of initial Cr(VI) concentration, in 25–95 mg l^{-1} range, on adsorption is studied and shown in figure 12. The initial Cr(VI) concentration provides driving force to overcome all mass transfer resistance of metal between aqueous and solid phase [38], thus, if initial Cr(VI) concentration increases from 25 to 100 mg l^{-1}, and Cr(VI) adsorption decreased from 92 to 50% (overall 45% reduction). At optimum 25 ppm concentration of Cr(VI), active binding sites gets unsaturated and offered large surface area for adsorption, but at higher concentration, accumulation of adsorbent particles escorts decrease total surface area is a cause for adsorption reduction with increasing initial Cr(VI) concentration gradient, matches to reported findings [35].

3.6 *Effect of contact time*

The effect of contact time on % removal has a linear impact over a span of 3 h and 75–80% increase in Cr(VI) ions adsorption observed in 180 min achieved at 200 rpm as shown in figure 13. Since, optimized contact time facilitates proper contact with composite binding sites to promote transfer of Cr(VI). At 120 and 150 rpm, Cr(VI) adsorption found slightly lower than optimized agitation time, 180 min, but adsorption found steady >180 min. These results indicate that contact between solid and liquid is more effective at agitation for 180 min (kept throughout experiments) agrees with reported results in literature Cr(VI) sorptions [38].

3.7 *Effect of agitation speed*

In batch adsorption systems, agitation speed plays a vital role affecting the external boundary film and the distribution of the metal ions in the bulk solution [22]. The effect of agitation speed on Cr(VI) adsorption examined at 100–300 rpm (figure 14). Cr(VI) adsorption found to be lower at agitation

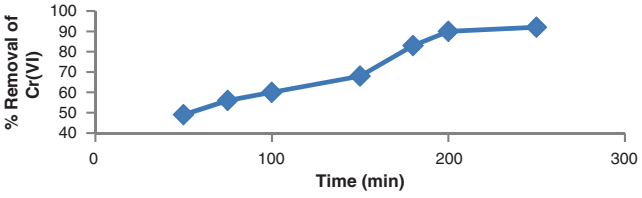

Figure 13. Effect of contact time on % removal of Cr(VI) ions (Cr(VI) concentration: 25 mg l^{-1}; temperature: 27°C; speed: 200 rpm; adsorbent: 5 g l^{-1}; pH 4).

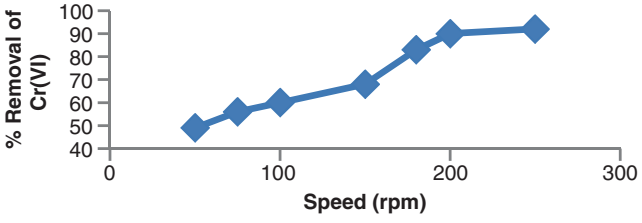

Figure 14. Effect of agitation speed on % removal of Cr(VI) ions (Cr(VI) concentration: 25 mg l^{-1}; temperature: 27°C; time 180 min; adsorbent: 5 g l^{-1}; pH 4).

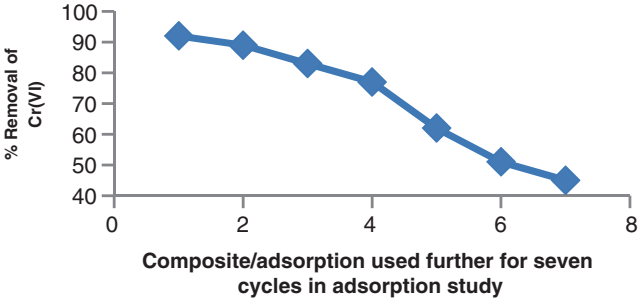

Figure 15. Regeneration of composite used in total seven cycles.

speed of 50, 100 and 150 rpm, but enhanced at 180 rpm and remains steady at >200 rpm. Cr(VI) removal efficiency not changed notably >200 rpm (optimal speed) as attributed to little resistance of boundary layer and high mobility of the system [39].

3.8 *Regeneration of adsorbent/composite*

Regeneration/desorption studies performed at pH = 8 are shown in figure 15. Initial electrostatic metal bindings onto amino/hydroxyl/active sites of chitosan composite gets weakened in basic pH due to competition with OH [35,40]. Literature too supports decreased Cr(VI) removal efficiency at pH > 7 presumably due to inactivity of proactive composite sites [32]. Above pH > 7, ions chemisorption gets decreased as chitosan undergoes deprotonation [35,41] and composite gets negatively charged above pH 7.5, so repelled/release off from composite [42].

GCB composite can be reused up to seven adsorption cycles with mere 44% reduction in Cr(VI) adsorption capacity and compared with other chitosan-based adsorbents in table 3.

3.9 *Sorption mechanism*

The metal Cr(VI) sorption onto GCB composite was screened to evaluate adsorption kinetics and isothermal analysis that is represented in table 2. The important kinetic constants were calculated by applying pseudo 1st order, 2nd order and intraparticle diffusion models using equations

Table 3. Adsorption capacities of different adsorbents for chromium (VI) [35,38–40].

Adsorbents	Max. sorption capacity (mg g^{-1})	pH	Max. Cr(VI) ions (mg g^{-1})
Pure chitosan only	27.2	6	800
Cross-linked chitosan	50.0	5.0	1000
Metal-imprinted chitosan	51.0	5.5	1000
Chitosan cross-linked epichlorohydrin	52.3	5.5	1000
Metal chitosan epichlorohydrin	51.0	5.5	1000
GCB, this research study	153.8[a]	4.0	105

[a]Based on graphite (20%, w/w) on chitosan (corresponds to max. capacity of 105.4 mg g^{-1} GCB).

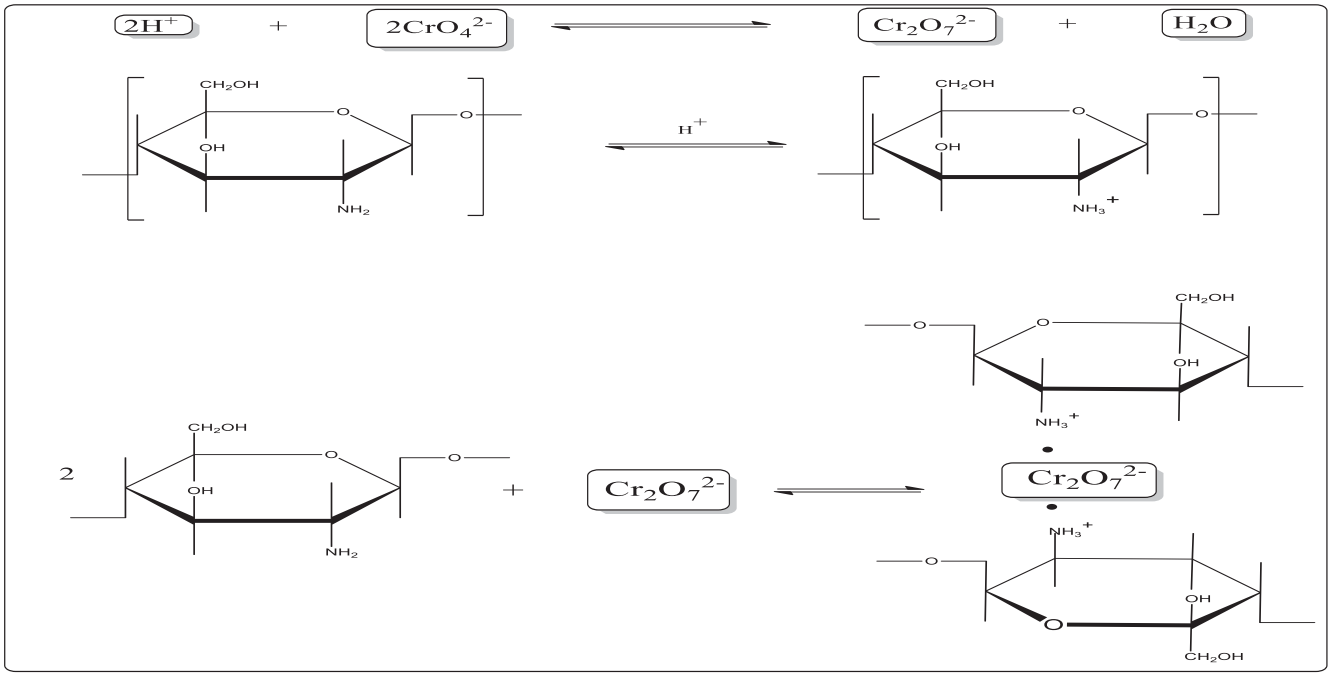

Figure 16. Mechanism of Cr(VI) sorption from water on GCB composite.

(4–9). The well-fitted Langmuir isotherm model showed an adsorption capacity (q_m) of 105.6 mg g^{-1} and $R^2 = 0.945$ suggested Cr(VI) sorption in GCB is a monolayer adsorption phenomena due to throughout homogeneous distribution of metal–composite coordination unit. Besides, rate of Cr(VI) adsorption is initially rapid, which then gradually gets steady with time (figure 14), and subsequently removal time is less for higher Cr(VI) ions concentration. The experimental adsorption capacity (q_e) found to be ∼105 mg g^{-1} for GCB composite as close to theoretical capacity that substantiates kinetics fitted well with the pseudo-second-order model as reported values by diverse materials [35]. This physical adsorption of Cr(VI) onto GCB has critically influenced under mild acidic conditions, i.e., pH = 4 favours and more efficient than neutral/higher pH as shown in figure 11 and also highlighted in reports [35]. This is due to pH dependency of varied Cr(VI) anionic species present in aqueous solution as chromate ion on lowering pH = 4 changes to orange colour dichromate ion which is subsequently grabbed by protonated $–NH_3^+/OH_2^+$ groups of GCB as shown in figure 16.

4. Conclusions

This study reported an efficient reductive removal of toxic Cr(VI) ions from aqueous solution employing easily synthesized GCB composite. The study was carried out by varying parameters viz., initial Cr(VI) ions, adsorbent dose, pH, agitations speed, contact time and adsorption models. The pseudo second-order kinetics and Langmuir model were best suited to describe adsorption equilibrium. The –OH, $–NH_2$ and –C–O–C functionalities of chitosan gets inter-wined with graphite in GCB composite exchanges. Cr(VI) anions from water with removal capacity of 105 mg g^{-1} found at pH ∼ 4, achieved in 3 h. The removal mechanism has also been demonstrated and GCB composites were reused in seven-fold cycle. Therefore, GCB is efficient matrix for the reductive removal of environmentally toxic and hazardous Cr(VI) as newer approach towards remediation of heavy metals from wastewater.

Acknowledgements

I am thankful for the supports from Head of the department of chemistry; RTM Nagpur University, Nagpur, to carry out this research and to Ms Asha H Gedam for graphical work. Compliance with ethical standards research involved no human participants and/or animals.

References

[1] Kortenkamp A, Shayer R O and Woodbrige N 1996 *Arch. Biochem. Biophys.* **329** 199

[2] Giwa A A, Olajire A, Oladipo M A, Bello M O and Bello I A 2013 *Inter. J. Sci. Eng. Res.* **4** 1275

[3] Nieboer E, Jusys A A, Nriagu J O and Nieboer E 1999 *Biologic chemistry of chromium,* in: *Chromium in Natural and Human Environments* (New York: Wiley Inter-Science) p 3

[4] U.S. EPA 1990 Draft manual of practice identification of illicit connections U.S. EPA Permits Division (EN-336)

[5] Yan G and Viraraghavan T 2001 *Biores. Technol.* **78** 243

[6] Benito Y and Ruiz M L 2002 *Desalination* **142** 229

[7] Volesky B and Holan Z R 1995 *Biotech. Prog.* **11** 235

[8] Xiaoqi S, Bo P, Ji C and Deqian C L 2009 *Am. Inst. Chem. Eng.* **55** 2062

[9] Peter M, Binulal N S, Soumya S, Nair S V, Furuike T, Tamura H *et al* 2010 *Carbohydr. Polym.* **79** 284

[10] Gandhi M R, Viswnathn N and Meenakshi S 2010 *Int. J. Biol. Macromol.* **47** 146

[11] Xi F, Wu J and Lin J X 2006 *J. Chroma* **1125** 38

[12] Crini G and Badot P M 2008 *Prog. Polym. Sci.* **33** 399

[13] Synowiecki J and Al-Khateeb N A 2003 *Crit. Rev. Food Sci. Nutri.* **43** 145

[14] Azlan K, Wan-Saime W N and Lai-Ken L 2009 *J. Environ. Sci.* **21** 296

[15] Fitzer E 1987 *Carbon* **25** 163

[16] Chauhan A, Chauhan P and Kaith B 2012 *J. Chem. Eng. Process. Technol.* **3** 1

[17] Eaton A D, Clesceri L S and Greenberg A E 1995 *Standard methods for the examination of water and wastewater*, 19th edn. (Washington: American Public Health Association) p 1325

[18] AOAC 1990 *Method of analysis*, 15th edn. (Washington: Association of Analytical Chemist) p 312

[19] Black C A 1965 *Methods of soil analysis. Part I: Physical and mineralogical properties.* (Madison: Wisconsin American Society of agronomy) p 671

[20] Wan Ngah W S, Kamari A, Fatinathan S and Ng P W 2006 *Adsorption* **12** 249

[21] Qian S, Huang G, Jiang J, He F and Wang Y 2000 *J. Appl. Polym. Sci.* **77** 3216

[22] Yeh J T, Chen C L and Huang K S 2007 *Mater. Lett.* **61** 1292

[23] Yen M T, Yang J H and Mau J L 2009 *Carbohydr. Polym.* **75** 15

[24] Trimukhe K D and Varma A J 2008 *Carbohydr. Polym.* **71** 698

[25] Kong L, Gao Y, Gong Y, Zhao N and Zhang X 2005 *J. Biomed. Mater. Res.* **75** 275

[26] Irfan M, Yim J H, Kim C and Jho Y D 2013 *Appl. Phys. Lett.* **103** 201108

[27] Ebru G, Dilay P, Cuney H, Unlu O A and Nurfer G 2007 *Carbohydr. Polym.* **67** 358

[28] Chong K H and Volesky B 1995 *Biotech. Bioeng.* **47** 451

[29] Langmuir I 1918 *J. Am. Chem. Soc.* **40** 1361

[30] Schmuhl R, Krieg K M and Keizer K 2001 *Water SA* **27** 1

[31] Batista A C L, Villanueva E R and Campos T G M 2011 *Molecules* **16** 3569

[32] Aydın Y A and Aksoy N D 2009 *Chem. Eng. J.* **151** 188

[33] Weber T W and Chakkravorti R K 1974 *AICHE J.* **20** 228

[34] Greenwood N N and Earnshaw A 1988 *Chemistry of elements* (New York: Pergamon; Springer Verlag Press) p 626

[35] Jung C, Heo J, Han J, Her N, Lee S J, Oh J *et al* 2013 *Separ. Purif. Technol.* **106** 63

[36] Luo C, Tian Z, Yang B, Zhang L and Yan S 2013 *Chem. Eng. J.* **234** 256

[37] Niyogi S, Abraham E T and Ramakrishana S V 1998 *J. Sci. Indus. Res.* **57** 809

[38] Gogate P R and Pandit A B 2004 *Adv. Environ. Res.* **8** 553

[39] Singanan M and Singanan V 2007 *Electro. J. Environ. Agri. Food Chem.* **6** 2557

[40] Bai A, Sudha R and Emilia A 2003 *Biores. Technol.* **87** 17

[41] Redlich O and Peterson D L 1959 *J. Phys. Chem.* **63** 1024

[42] Huang R, Yang B and Liu Q 2013 *Appl. Polym. Sci.* **129** 908